Numerically-Simulated Exposure of Children and Adults to Pulsed Gradient Fields in MRI

Amine M. Samoudi[*1], MS, Günter Vermeeren[1], PhD, Emmeric Tanghe[1], PhD, Roel Van Holen[2], PhD, Luc Martens[1], PhD, and Wout Joseph[1], PhD

[1]Department of Information Technology (INTEC), Ghent University/iMinds, iGent, Technologiepark-Zwijnaarde 15, 9052 Ghent, Belgium

[2]Electronics and Information Systems (ELIS), Ghent University/iMinds, Campus Heymans - Block B, De Pintelaan 185 , B-9000 Gent, Belgium

[*]Correspondence to: Amine M. Samoudi, MS. Department of Information Technology (INTEC), Ghent University/iMinds, iGent, Technologiepark-Zwijnaarde 15, 9052 Ghent, Belgium.
E-mail: amine.samoudi@intec.ugent.be

Grant sponsor: This work was supported by the iMinds SIMRET ('SImultaneous Magnetic Resonance imaging and Emission Tomography') project, co-funded by iMinds, a research institute founded by the Flemish Government in 2004, and the involved companies and institutions.

Running title: Exposure of Patients to Gradient Fields

ABSTRACT

Purpose: To determine exposure to gradient switching fields of adults and children in a magnetic resonance imaging(MRI) scanner by evaluating internal electric fields within realistic models of adult male, adult female, and child inside transverse and longitudinal gradient coils, and to compare these results with compliance guidelines.

Materials and Methods: Patients inside x-, y-, and z-gradient coils were simulated using anatomically realistic models of adult male, adult female, and child. The induced electric fields were computed for 1 kHz sinusoidal current with a magnitude of 1 A in the gradient coils. Rheobase electric fields were then calculated and compared to the ICNIRP 2004 and IEC 2010 guidelines. Effect of the human body, coil type, and skin conductivity on the induced electric field was also investigated.

Results: The internal electric fields are within the first level controlled operating mode of the guidelines and range from $2.7Vm^{-1}$ to $4.5Vm^{-1}$, except for the adult male inside the y-gradient coil (induced field reaches $5.4Vm^{-1}$).The induced electric field is sensitive to the coil type (electric field in the skin of adult male: $4\mathrm{Vm}^{-1}$, $4.6\mathrm{Vm}^{-1}$, and $3.8\mathrm{Vm}^{-1}$ for x-, y-, and z-gradient coils, respectively), the human body model (electric field in the skin inside y-gradient coil: $4.6\mathrm{Vm}^{-1}$, $4.2\mathrm{Vm}^{-1}$, and $3\mathrm{Vm}^{-1}$ for adult male, adult female, and child, respectively), and the skin conductivity (electric field $2.35\%-4.29\%$ higher for $0.1\mathrm{Sm}^{-1}$ skin conductivity compared to $0.2\mathrm{Sm}^{-1}$).

Conclusion: The y-gradient coil induced the largest fields in the patients. The highest levels of internal electric fields occurred for the adult male model.

Key words: MRI; exposure; ICNIRP; IEC; Induced electric field; Peripheral Nerve Stimulation.

INTRODUCTION

Interactions of the living tissue with MRI scanner can cause potential patient risks (1–3). Rapidly induced fields could stimulate nerves of the peripheral nervous system (PNS) (3,4). Nerve stimulation might interfere with the examination (5). Therefore, the physiological limit of exposure to such fields should be based on minimizing uncomfortable or intolerable sensation. Different guidelines and standards (5–7) suggest limits to mitigate these potential hazards. The IEC (2010) and ICNIRP (2004) recommended a maximum exposure level be set to a time rate of change of the magnetic field (dB/dt) or induced electric field (E) of 80% of the median perception threshold for peripheral nerve stimulation for routine operation, and 100% of the median perception threshold for controlled operation (5,7).

Bencsik et al. (8) used spherical and cylindrical tissue models to study the induced electric fields due to gradient fields. Mao et al. (9) used the visible male model within an unshielded single-axis (x-axis) gradient and reported calculations of the induced E-field within in the presence of RF shield. Zhao et al. (10) used a modified finite difference time domain technique to simulate the induced electric field and current density within adult male model. So et al. (11) investigated the peripheral nerve stimulation by unshielded y- and z- gradient coils using an average size male model. Only male or simplified human models were used for these investigations in the majority of the cases. Another important issue is the modeling of the skin in the low-frequency magnetic field exposure. Schmid et al. (12) pointed out an obvious potential source of errors and uncertainties concerning computations of induced electric field strengths inside skin tissue in the low frequency range. It has been demonstrated that the conductivity values for skin obtainable from the most widely used data bases of dielectric tissue properties are not suitable for exposure assessment with respect to peripheral nerve tissue. Recently, De Santis et al. (13) conducted a sensitivity analysis on the electro-

geometrical parameters of human skin. First, a multi-layer canonical skin structure is modeled to closely mimic the biological composition of the skin. An equivalent single-layer skin model is then derived. They finally suggested the value of 0.2 S/m for the skin conductivity. The purpose of the present study is to determine exposure of adults and children in an MR scanner by evaluating the induced electric fields in realistic 3D whole-body adult male, adult female, and child models within shielded whole-body x-, y-, and z-gradient coil and compare them with ICNIRP 2004, and IEC 2010 guidelines.

MATERIALS AND METHODS

Simulation platform

Gradient coils and human models were modeled with a commercial software package SEMCAD-X (14). The induced electric fields in the human body were analyzed with the SEMCAD X magneto quasi-static solver.

Gradient coils models

Whole-body, symmetric shielded gradient transverse (x- and y-axis) and longitudinal (z-axis) coils (15) were used in this investigation to compute the current densities and the electric fields induced in the body models. All three gradient coils have approximately the same axial length of 1.4 m and the same diameter of 0.6 m for the primary coils. With this axial length, the gradient coils would fit inside most conventional MRI systems ((16,17)). Table 1 lists some coils parameters while Fig. 1 shows designs of the gradient coils. The gradient coils are fed with pulsed sine currents of 1 kHz.

Anatomical models and tissue dielectric properties

We used three human models (Figure 2) from the Virtual Population (18): Duke, a 34-year-old male (72 kg, 1.77 m); Ella, a 26-year-old female (59 kg, 1.63 m); and Billie, an 11-year-old girl (35 kg, 1.47 m). These anatomical models have been developed from high-resolution MRI data and consist of more than 80 tissues and organs (19). The dielectric parameters of the tissues are set based on the database developed by the IT'IS Foundation (19) mainly from the Gabriel dispersion relations (20). To further account for weighing outer and inner skin layers, skin conductivity has been set to 0.2 S m^{-1} (13). The effect of skin conductivity on

the induced electric field was investigated by comparing results using skin conductivity of 0.1 S m^{-1} and 0.2 S m^{-1}.

The human models are centered inside the gradient coils as shown in Figure 2. Uniform rectilinear meshes were applied to easily discretize the complex anatomical models with a voxel size of 2 mm along x, y, and z direction.

Comparison with analytical solutions

We performed simulations to compare analytically derived results with simulations results to verify the simulation platform. The numerical model is composed of a homogeneous sphere (conductivity = 0.1 S m^{-1}, radius = 0.25 m) placed symmetrically inside two concentric current loops forming a Helmholtz pair with radius and center-center separation of 0.35 m (Fig. 3a). The two loops were fed with a sinusoidal current of peak amplitude 1 A and the model was discretized with a voxel size of 5 mm. The B-field at a distance r off axis in the mid-plane, B_{Hz} is (21,22):

$$B_{Hz} = \frac{I\mu_0}{\pi a\sqrt{((1+\alpha)^2+\beta^2)}} \times [E(k)\ \frac{1-\alpha^2-\beta^2}{(1+\alpha)^2+\beta^2-4\alpha} + K(k)] \quad (1)$$

where *I* is the current in the loops, a is the radius of the loops, α = r/a, β = d/a, $k = \frac{2\sqrt{ar}}{a+r}$, r is the radial distance from the axis to the field measurement point, 2d is the separation of the loops, and *E(k)* and *K(k)* are the complete elliptical integrals of the first and second kind, respectively.

Analytical formula of the current density within a homogeneous sphere exposed to a time-varying uniform B-field is given (22):

$$J(r) = \pi f \sigma B r \quad (2)$$

where r is the radial distance (m), f is the frequency (Hz), B is the magnetic flux density (T), and σ is the conductivity (S m^{-1}).

Evaluation of the induced electric field

To make a fair comparison possible with the previous published works, all the simulations were performed for 1 kHz sinusoidal current with a magnitude of 1 A in the longitudinal and the transverse gradient coils. For the frequency and current considered, the computed electric fields are scaled as follows (11):

$$E_{Rh} = E_{1kHz} \frac{(\frac{dB}{dt})_{Rh}}{(\frac{dB}{dt})_{1A}} \quad (3)$$

Where E_{Rh} is the rheobase electric field, E_{1kHz} is the extracted field at 1 kHz, $(^{dB}/_{dt})_{Rh}$ is the rheobase time derivative of magnetic flux assumed to be equal to 18.8 T/s for x- and y-gradient coil, and equal to 28.8 T/s for z-gradient coil according to the ICNIRP 2004 on medical magnetic resonance: protection of patients (5), and $(^{dB}/_{dt})_{1A}$ is the time derivative of the magnetic field at 0.2 m off the coil center for unit coil current through the coil as specified by the IEC 2010 (7) and is equal to (for 1 kHz sinusoidal):

$$(\frac{dB}{dt})_{1A} = 2\pi 10^3 B_{max,1A} \quad (4)$$

$B_{max,1A}$ is the maximum magnetic flux density for a 0.2 m radius cylinder with unit current in the coil.

We used the ICNIRP 2010 (23) approach to determine the induced electric field *E* (r_0) at a location r_0 as a vector average within a small contiguous tissue cubic volume of 2×2×2 mm^3 of the electric field $E(r)$. More specifically:

$$< E(r_0) >_V = \frac{1}{V} \int_V E(r)\, dv \tag{5}$$

where $0 < V \leq 8$ mm^3 is the volume of lossy tissue within the cube. To comply with the 2×2×2 mm^3 average volume, no averaging will be performed at a voxel if the cube is not completely within the tissue of interest, and the E-field value of this voxel will not be considered as a spatially averaged value. We also used the 99th percentile value of the electric field for a specific tissue as suggested by the ICNIRP 2010.

The IEC:2010 60601-2-33 standard and the ICNIRP statement on medical magnetic resonance procedures: protection of patients (2004) prescribes the following limits related to PNS for the induced electric field in the normal operating mode (L_{01}) and in the first level controlled operating mode (L_{12}):

$$L_{01} = 0.8 * 2.2 \frac{V}{m} * (1 + \frac{0.36\ ms}{t_{s,eff}}) \tag{6}$$

$$L_{12} = 1.0 * 2.2 \frac{V}{m} * (1 + \frac{0.36\ ms}{t_{s,eff}}) \tag{7}$$

Where $t_{s,eff}$ denotes the effective stimulus duration, which is defined as

$$t_{s,eff} = \frac{\sin^{-1}(0.8)}{\pi * f} \tag{8}$$

for sinusoidal waveforms of frequency f. This leads to $L_{01} = 3.9\ \mathrm{V}\, m^{-1}$ and $L_{12} = 4.9\ \mathrm{V}\, m^{-1}$.

RESULTS

Verification of low-frequency solver

Figure 3b shows the simulated and analytically-derived current density within the homogenous sphere for different radial distances in z = 0 plane. Using Eq. (1) and Eq. (2), taking σ = 0.1 S m^{-1}, f = 1 kHz, it follows that the numerical values simulated at 1 kHz deviate with 0.53-0.93 % from the analytical value, indicating excellent agreements between simulations and analytical results. We observe that the simulated value tends to overestimate slightly the analytical value due to the spatial variation the B-field produced by the Helmholtz pair.

Induced electric field in the body-Effect of coil type

Table 2 shows the calculated electric field in fat and skin (where peripheral nerves are located) for different coils, and Figure 4 shows the distribution of the in-situ electric field. Several observations can be made based on the Table 2. The induced electric field is higher in transverse coils (x and y gradient coils) than in longitudinal coil (z gradient coil) despite stronger magnetic flux density produced by the longitudinal coil (e.g. E_{max} Duke, skin: 186 $mV\,m^{-1}$, 197 $mV\,m^{-1}$, and 143 $mV\,m^{-1}$ for x, y, and z gradient coils, respectively). Results also show that difference between transverse and longitudinal coil is more visible in the E_{max} than in the $E_{99\%}$ (difference of 18.5 % to 48 % for E_{max} compared to a difference of 10.1 % to 16.7 % for $E_{99\%}$). We also observe that all the electric fields simulated are greater in fat than in skin.

Induced electric field in the body-Effect of model type

The influence of the body model is illustrated in Table 2 and Figure 4. It is obvious from the table that the in-situ electric field is higher in Duke than in Ella and Billie for x, y, and z gradient coils and that the maximum induced field decreases with the decrease in the body size (e.g. $E_{99\%}$ fat inside y-gradient coil: 109 $mV\,m^{-1}$, 86 mVm^{-1}, and 61 mVm^{-1} for Duke, Ella, and Billie, respectively). Table 2 shows also that the difference between $E_{99\%}$ of fat and skin is tighter for Billie (child model) than for adult models. Localized high electric field values occur at the periphery of the volume occupied by the human body, as illustrated in Fig. 4.

Induced electric field in the body-Effect of skin conductivity

Table 3 shows E_{max} and $E_{99\%}$ for Duke inside x, y, and z gradient coils using the skin conductivity of 0.1 S m^{-1} and 0.2 $S\,m^{-1}$. The peak-induced E-field is higher for the skin conductivity of 0.1 $S\,m^{-1}$ compared to the skin conductivity of 0.2 $S\,m^{-1}$. This difference is highlighted in the E_{max} rather than in the $E_{99\%}$ value.

Rheobase electric field-Threshold for PNS

From Table 4 $B_{max,1A}$ is equal to 62.87 μT, 60.37 μT, and 84.39 μT, for x, y and z gradient coil, respectively. The given flux density is the maximum value within the volume of a cylinder with 0.2 m radius and a height of 0.2 m. Rheobase electric fields are computed from Tables 2 and 4 using (3). Calculations are summarized in Table 5. Table 5 shows that the E_{max} exceeds the standards basic restrictions for all the models and the coils (5.5 $V\,m^{-1}$ – 13.5 $V\,m^{-1}$). The $E_{99\%}$ is within the normal operating mode guidelines for the child model inside all the coils (2.7 $V\,m^{-1}$ – 3 m^{-1}) and the adult female inside x and z gradient coils

(3.3 $V\,m^{-1}$ – 3.8 $V\,m^{-1}$). The $E_{99\%}$ exceeds the normal operating mode guidelines but remains within the first level controlled operating mode for the adult female model inside y-gradient coil (4.2 $V\,m^{-1}$ – 4.3 $V\,m^{-1}$), and the adult male model inside x and z gradient coils (4.2 $V\,m^{-1}$ – 4.5 $V\,m^{-1}$). Only the $E_{99\%}$ of the Duke model inside the y-gradient coil exceeds the first level controlled operating mode ($E_{99\%} = 5.4\,V\,m^{-1}$).

DISCUSSION

Numerical simulations of E-field within a realistic model of adult male, adult female, and child located inside a generic shielded x-, y-, and z-gradient coil set have been presented and compared to the ICNIRP 2004 and IEC 2010 guidelines.

We verified the applied numerical technique (low frequency solver in SEMCAD) with an analytical solution for a conducting sphere centered inside a Helmholtz coil. The simulated current density in the mid-plane (z = 0) at different radial distances (from 0.01 m to 0.1 m) agreed with analytically-derived values with deviation less than 1%. We observe that the simulated value tends to overestimate slightly the analytical value due to the spatial variation of the B-field produced by the Helmholtz pair (formula of Eq. 2 assumed a time-varying uniform B-field while the Helmholtz B-field started lacking its uniformity when the radial distance r approaches 0.1 m for z = 0). The magneto quasi-static low-frequency solver of SEMCAD and its use in exposure investigations was also verified in several studies (9,24).

From Faraday's law, it follows that the largest values of circumferentially induced electric fields normal to the direction of applied magnetic field will localize in the outermost body surfaces (17). Since the body models are inhomogeneous in conductivity distribution due to different tissues, the current flow will be modified by this difference in dielectric parameters between tissues. Therefore, high values of induced internal electric field were notable on the front and lower back surfaces of the trunk with low internal electric field values in the middle of the body. It follows that the peripheral nerves in the skin are exposed to the strongest electric fields. The y-gradient coil induced larger internal electric fields. This is due to the fact that for y-gradient coil, the B-field in the body is oriented in the y-direction, and since the induced electric fields and circulating currents in materials are proportional to the radius of the loop (i.e. the cross-section of the body), the highest electric fields will be induced if the

magnetic field is oriented from front to back, which is in agreement with previously published works (25).

The electric field is greater in fat than in skin. This due to the conductivity being lower in the fat compared to the skin ($0.04\,S\,m^{-1}$ for fat and $0.2\,S\,m^{-1}$ for skin), and was already explained and reported in several published research (in general, tissues of lower conductivity have greater peak-electric field than high conductivity tissues induced in them by the same magnetic flux density (13,26)).

Our results show that the human body model and the body size in general, is a primary factor for the induced electric fields. The maximum induced field occurred for the largest size of the body model (Duke). This behavior was also reported in several studies of exposure to uniform magnetic field (see Ref. (27) for example). Differences in shape and anatomy between the models are also a factor affecting the induced field but remain less important than the size of the model.

The skin conductivity does not have a great impact on the induced electric field for the 99% value (as an averaged value) which is in agreement with the works of the De Santis et al. (13). They reported that any value of the skin conductivity between the range of 0.1–0.7 $S\,m^{-1}$ will not considerably alter the spatial average E-fields. However, the maximum electric field decreased with the skin conductivity value as reported and explained in (13,26).

Figure 4 indicates that the largest volumes of high intensity electric field are in the torso and in the outermost body surfaces, which is the body region where the greatest number of stimulations were reported by the subjects (28).

To make possible a fair comparison with previously published works, we used the $E_{99\%}$ as the main value (which is also the value used in the guidelines). Rheobase electric fields for

PNS computed in this paper are in the range of $2.7\ V\ m^{-1} - 5.4\ V\ m^{-1}$. These values are in agreement with published studies (11,25). In (25) , an averaged value of $E = 4.2\ V\ m^{-1}$ was reported and estimated $2.9\ V\ m^{-1} - 5.8\ V\ m^{-1}$ was reported in (11).

Compliance with the ICNIRP 2004 and IEC 2010 guidelines for the normal operating mode (L_{01}) guidelines was recorded for the child model inside all the coils and the adult female inside x and z gradient coils. Results for the adult female model inside y-gradient coil and the adult male model inside x and z gradient coils exceeded the L_{01}, but remained within the first level controlled operating mode (L_{12}). The $E_{99\%}$ of the adult male model inside the y-gradient coil exceeded the L_{01} and L_{12} by a factor of 1.38 and 1.1 respectively.

We note that we have focused on the configuration of human bodies centered with respect to the coils; the sensitivity of the PNS sensation thresholds to the human body position was already investigated by (11,28). So et al. concluded that the position of the human body inside the coils influences the magnitude of the induced electric field. The changes, however, are typically below 20% for most measures and less than 5% for the average value of the electric field for a given tissue in a given coil (11). We believe that a sensitivity study concerning the effect of the human body's position inside the coils on the induced electric field using great populations span will clarify more this point and add more results about the PNS thresholds. The proposed work does not consider the effect of coupling of the gradient and/or RF coils, nor the additional induced electric field due to gradient coils' eddy currents (29,30), which leads to some remnant errors. Another source of uncertainty is the fact that the body is highly nonlinear medium with dielectric properties of each and every person different, and thus it is quite difficult to predict the exact mechanisms of induced fields and their effects on the physiology.

In conclusion, in this study we have modeled the exposures of male, female and child patients to pulsed gradient fields typically used in MRI systems. These gradients coils are intended to be models of currently available cylindrical MRI systems, but we do not claim that we covered all gradient sets on the market and therefore we provided indicative results only. The y-gradient tends to induce more fields in the models than the other coils. The strongest levels of field exposure are observed for the adult male inside the y-gradient coil. The internal electric fields, when the patients are inside the gradient coils are within the first level controlled operating mode of the ICNIRP 2004 and IEC 2010 guidelines, except for the adult male inside the y-gradient coil. Further work will consist of the investigation of different postures and positions within the coils. Investigations such as these will help inform compliance of clinical procedures.

ACKNOWLEDGMENTS

We would like to thank Michael Poole for his help with the gradient coil design.

REFERENCES

1. Schenck JF. Physical interactions of static magnetic fields with living tissues. Prog Biophys Mol Biol. 2005;87(2-3 SPEC. ISS.):185–204.

2. Shellock FG. Radiofrequency energy-induced heating during MR procedures: A review. J Magn Reson Imaging. 2000;12(1):30–6.

3. Schaefer DJ, Bourl JD, Bourland JD, Nyenhuis JA. Review of patient safety in time-varying gradient fields. J Magn Reson Imaging. 2000;12(1):20–9.

4. Reilly JP. Peripheral nerve stimulation by induced electric currents: exposure to time-varying magnetic fields. Med Biol Eng Comput. 1989;27(March):101–10.

5. ICNIRP (International Commission on Non-ionising Radiation Protection), Medical magnetic resonance (MR) procedures: protection of patients. Heal Phys. 2004;87:197–216.

6. IEEE standard for safety levels with respect to human exposure to electromagnetic fields, 0–3 kHz, C95.6-2002, New York: Institute of Electrical and Electronics Engineers. 2002;43.

7. IEC (Edition 3.0 2010) 60601-2-33 Medical electrical equipment – Part 2–33: Particular requirements for the basic safety and essential performance of magnetic resonance equipment for medical diagnosis.

8. Bencsik M, Bowtell R, Bowley RM. Using the vector potential in evaluating the likelihood of peripheral nerve stimulation due to switched magnetic field gradients. Magn Reson Med. 2003;50:405–10.

9. Mao W, Chronik B a., Feldman RE, Smith MB, Collins CM. Consideration of

magnetically-induced and conservative electric fields within a loaded gradient coil. Magn Reson Med. 2006;55(December 2005):1424–32.

10. Zhao H, Crozier S, Liu F. Finite difference time domain (FDTD) method for modeling the effect of switched gradients on the human body in MRI. Magn Reson Med. 2002;48(6):1037–42.

11. So PPM, Stuchly M a., Nyenhuis J a. Peripheral nerve stimulation by gradient switching fields in magnetic resonance imaging. IEEE Trans Biomed Eng. 2004;51(11):1907–14.

12. Schmid G, Cecil S, Überbacher R. The role of skin conductivity in a low frequency exposure assessment for peripheral nerve tissue according to the ICNIRP 2010 guidelines. Phys Med Biol. 2013;58(13):4703–16.

13. Santis V De, Chen XL, Laakso I, Hirata A. An equivalent skin conductivity model for low-frequency magnetic field dosimetry. Biomed Phys Eng Express. IOP Publishing; 2015;1(1):015201.

14. SEMCAD X. Simulation platform for electromagnetic and thermal dosimetry, Schmid & Partner Engineering AG, Switzerland, Available online at www.semcad.com; visited on January 2016.

15. Poole M, Bowtell R. Novel gradient coils designed using a boundary element method. Concepts Magn Reson. 2007;B31:162–75.

16. NHS Purchasing and Supply Agency. Report 06006 3T MRI Systems. 2007.

17. Crozier S, Wang H, Trakic A, Liu F. Exposure of workers to pulsed gradients in MRI. J Magn Reson Imaging. 2007;26(5):1236–54.

18. Christ A, Kainz W, Hahn EG, Honegger K, Zefferer M, Neufeld E, et al. The Virtual Family--development of surface-based anatomical models of two adults and two children for dosimetric simulations. Phys Med Biol. 2010;55(2):N23–38.

19. Hasgall P, Neufeld E, Gosselin M, Klingenböck A, Kuster N. 2012. IT'IS database for thermal and electromagnetic parameters of biological tissues. www.itis.ethz.ch/database [last accessed January 2016].

20. Gabriel C. 1996. Compilation of the dielectric properties of body tissues at RF and microwave frequencies. Technical Report AL/OE-TR-1996-0037, Occupational and Environmental Health Directorate. Radiofrequency Radiation Division, Brooks Air Force Base, Texas.

21. Montgomery DB, Terrell, J. Some useful information for the design of air core solenoids. National Magnet Laboratory, M.I.T. Report. AFOSR-1525, November 1961.

22. Smythe WR. Static and Dynamic Electricity, 2nd. New York:McGraw-Hill; 1968. p 266.

23. ICNIRP. International Commission on Non-Ionizing Radiation Protection, Guidelines for limiting exposure to time-varying electric and magnetic fields (1 Hz to 100 kHz). Heal Phys. 2010;99(6):818–36.

24. Bakker JF, Paulides MM, Neufeld E, Christ a, Chen XL, Kuster N, et al. Children and adults exposed to low-frequency magnetic fields at the ICNIRP reference levels: theoretical assessment of the induced electric fields. Phys Med Biol. 2012;57(7):1815–29.

25. Liu F, Zhao H, Crozier S. On the induced electric field gradients in the human body

for magnetic stimulation by gradient coils in MRI. IEEE Trans Biomed Eng. 2003;50(7):804–15.

26. Stuchly MA, Dawson TW, Member S. Interaction of Low-Frequency Electric and Magnetic Fields with the Human Body. 2000;88(5):643–64.

27. Caputa K, Dimbylow PJ, Dawson TW, Stuchly MA. Modelling fields induced in humans by 50/60 Hz magnetic fields: reliability of the results and effects of model variations. Phys Med Biol. 2002;47:1391–8.

28. Nyenhuis JA, Bourland JD, Kildishev A V, Scaefer DJ. Health effects and safety of intense MRI gradient fields. Magnetic Resonance Procedures: Health Effects and Safety, 1 ed, F. G. Shellock, Ed. Cleveland, OH: CRC. 2001. 31-52 p.

29. Samoudi AM, Van Audenhaege K, Vermeeren G, Poole M, Tanghe E, Martens L, et al. Analysis of Eddy Currents Induced by Transverse and Longitudinal Gradient Coils in Different Tungsten Collimators Geometries for SPECT/MRI Integration. Magn Reson Med. 2015;74:1780–9.

30. Samoudi AM, Van Audenhaege K, Vermeeren G, Verhoyen G, Martens L, Van Holen R, et al. Simulated Design Strategies for SPECT Collimators to Reduce the Eddy Currents Induced by MRI Gradient Fields. IEEE Trans Nucl Sci. 2015;62(5):2017–22.

Tables

Table 1

Geometrical parameters of the transverse and the longitudinal gradient coils*

Coil	Primary coil diameter (m)	Secondary coil diameter (m)	Primary coil length (m)	Secondary coil length (m)	DSV (m)
x-gradient	0.6	0.75	1.4	1.75	0.29
y-gradient	0.6	0.75	1.4	1.75	0.27
z-gradient	0.6	0.76	1.4	1.74	0.36

*The diameter of spherical volume (DSV) is given as the region where the gradient field is uniform to 5% peak-peak and is expressed as diameter in meters.

Table 2

Calculated electric fields (mV m^{-1}) in fat and skin of the body models (1-A current into coil at 1 kHz)

Model	***Coil***	***Tissue***	$E_{max}\ (mV\,m^{-1})$	$E_{99\%}\ (mV\,m^{-1})$
Duke	**x-coil**	Fat	242	94
		Skin	186	85
	y-coil	Fat	272	109
		Skin	197	92
	z-coil	Fat	152	78
		Skin	143	70
Ella	**x-coil**	Fat	221	79
		Skin	149	72
	y-coil	Fat	248	86
		Skin	172	84
	z-coil	Fat	139	63
		Skin	133	60
Billie	**x-coil**	Fat	179	59
		Skin	116	57
	y-coil	Fat	191	61
		Skin	130	60
	z-coil	Fat	110	54
		Skin	106	52

Table 3

Calculated electric fields (mV m^{-1}) in fat and skin for Duke model using skin conductivity of 0.1 S m^{-1} and 0.2 S m^{-1} (1-A current into coil at 1 kHz)

Model	***Coil***	***Tissue***	$E_{max}\ (mV\,m^{-1})$	$E_{99\%}\ (mV\,m^{-1})$
Duke	**x-coil**	Skin (0.1 S m^{-1})	198	87
		Skin (0.2 S m^{-1})	186	85
	y-coil	Skin (0.1 S m^{-1})	215	96
		Skin (0.2 S m^{-1})	197	92
	z-coil	Skin (0.1 S m^{-1})	154	73
		Skin (0.2 S m^{-1})	143	70

Table 4

Maximum magnetic flux density (μT) in the gradient coils in cylinder of r = 0.2 m in the center of the coils.

	x-coil	**y-coil**	**z-coil**
$\boldsymbol{B_{max}}$ **(μT)**	62.87	60.37	84.39

Table 5

Rheobase electric fields (V m^{-1})

Model	***Coil***	***Tissue***	$E_{max}\ (V\,m^{-1})$	$E_{99\%}\ (V\,m^{-1})$
Duke	**x-coil**	Fat	11.5	4.5
		Skin	8.9	4
	y-coil	Fat	13.5	5.4
		Skin	9.8	4.6
	z-coil	Fat	8.3	4.2
		Skin	7.8	3.8
Ella	**x-coil**	Fat	10.5	3.8
		Skin	7.1	3.4
	y-coil	Fat	12.3	4.3
		Skin	8.5	4.2
	z-coil	Fat	7.6	3.4
		Skin	7.2	3.3
Billie	**x-coil**	Fat	8.5	2.8
		Skin	5.5	2.7
	y-coil	Fat	9.5	3
		Skin	6.4	3
	z-coil	Fat	6.0	2.9
		Skin	5.8	2.8

Figure Legends

Figure 1. a: Wire patterns for a: x-gradient coil, b: y-gradient coil, and c: z-gradient coil. For transverse coils only one primary and one secondary layer is illustrated, while both are plotted for the longitudinal gradient coil.

Figure 2. Orthogonal views (front and side) of body model inside gradient coils. a, b: Duke inside the x gradient coil. c, d: Ella inside the y gradient coil. e, f: Billie inside the z gradient coil.

Figure 3. a: Homogenous sphere (conductivity 0.1 S m^{-1}) of radius 0.25 m positioned symmetrically between two concentric current loops forming a Helmholtz pair. The radii of the loops and their center-center separation were 0.35 m. b: Comparison of simulated and analytically derived current density in z = 0 plane against the radial distance r in (m).

Figure 4. Distribution of the internal electric field E_i (dB normalized to 272 mV m^{-1}) for different gradient exposure (from top to bottom : x, y, z, gradients coils) in the Duke, Ella, and Billie models, in the coronal planes y = -0.0215 m, y = -0.026 m, and y = -0.015 m for Duke, Ella, and Billie, respectively.

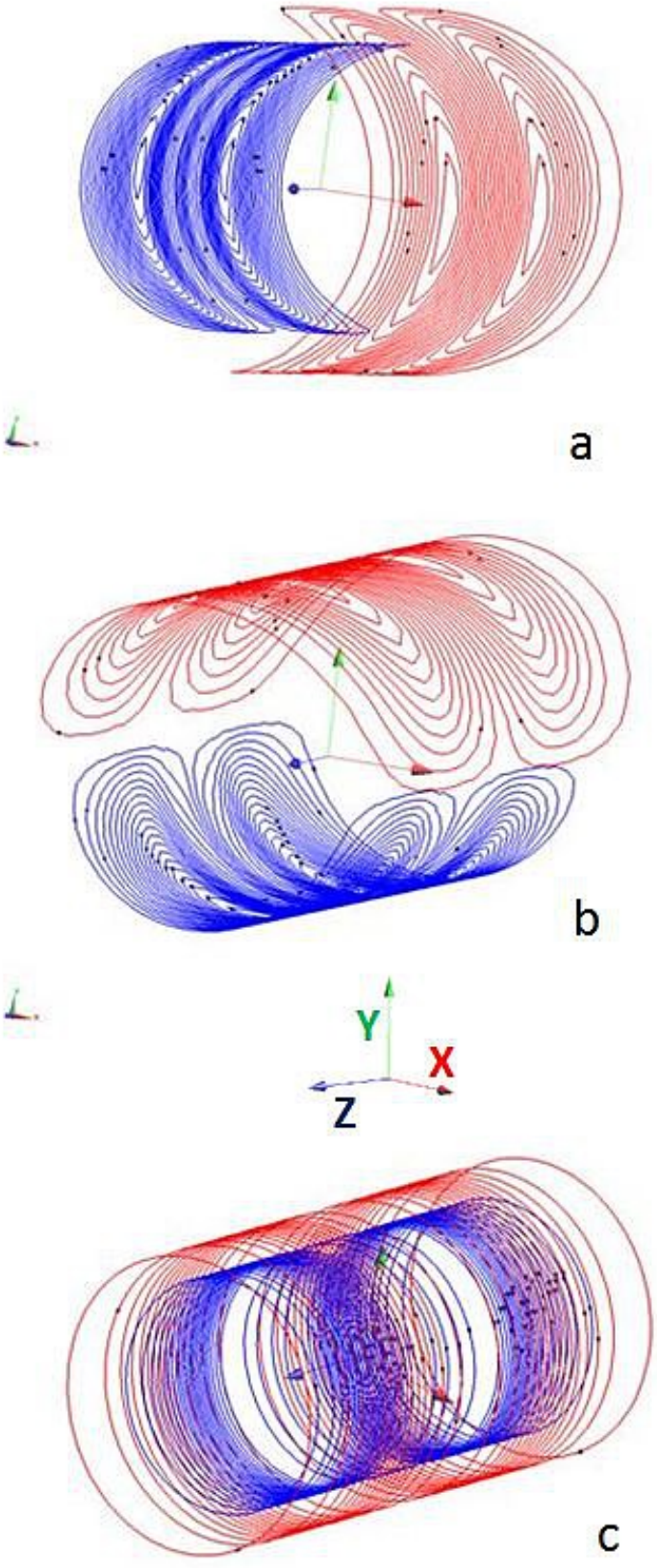

Figure 1

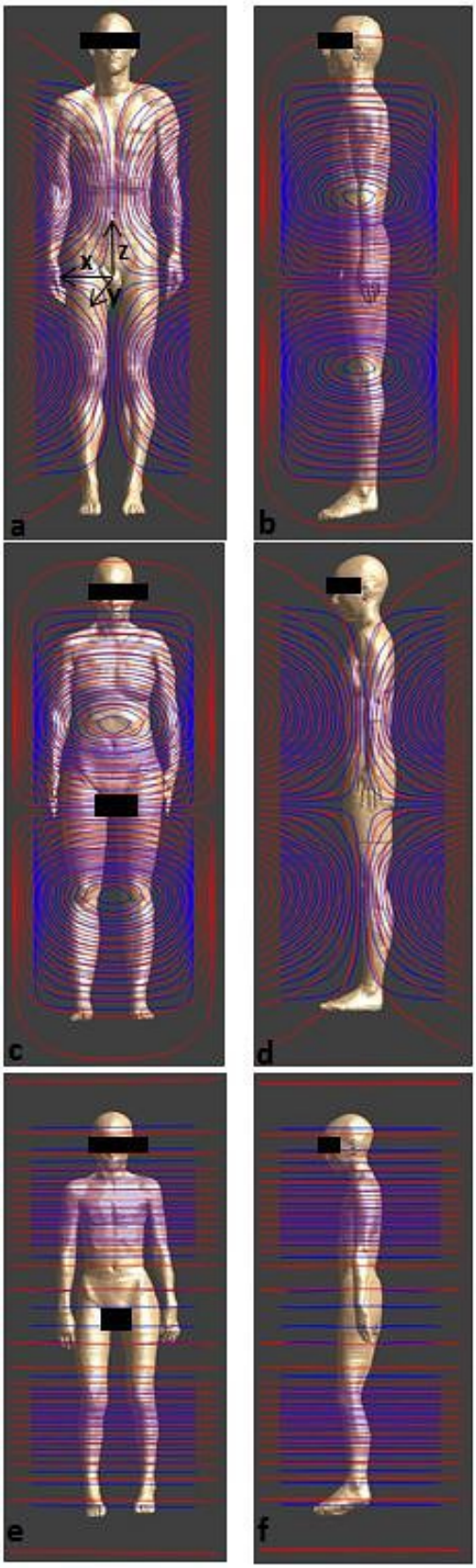

Figure 2

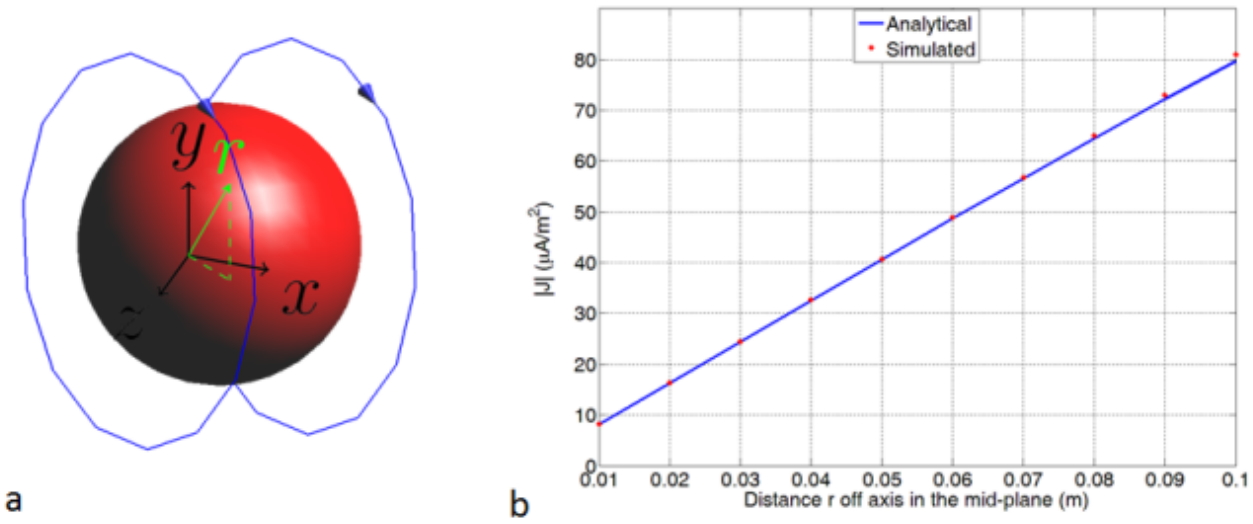
y
r
x
z
a
Analytical
Simulated
|J| (μA/m²)
0
10
20
30
40
50
60
70
80
0.01
0.02
0.03
0.04
0.05
0.06
0.07
0.08
0.09
0.1
Distance r off axis in the mid-plane (m)
b

Figure 3

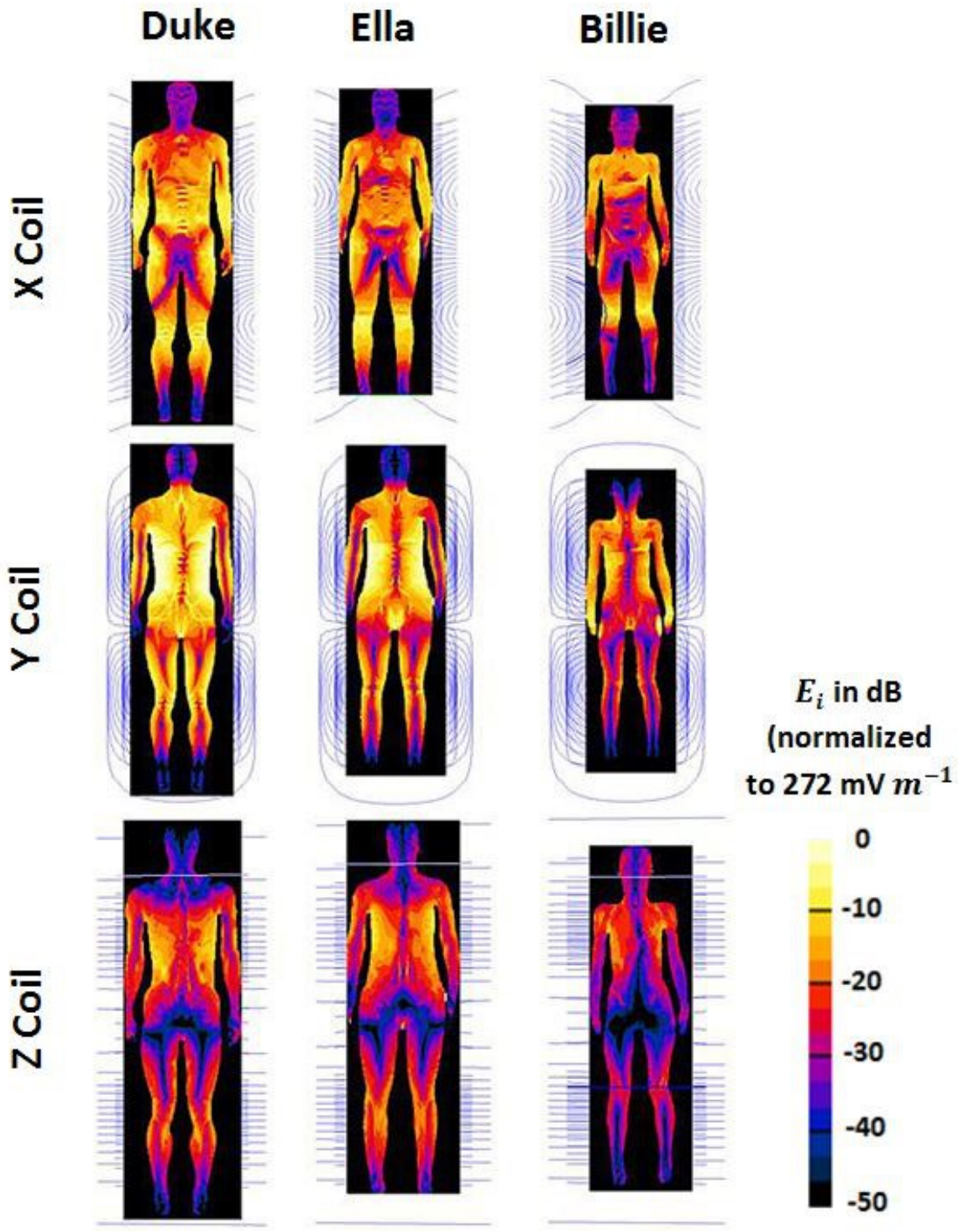
Duke
Ella
Billie
X Coil
Y Coil
Z Coil
E_i in dB
(normalized
to 272 mV m^{-1}
0
-10
-20
-30
-40
-50

Figure 4